

Tomographic Imaging of the Distal Extremities Using Cone-Beam Collimation

Jeffrey A. Cooper, Mubashar M. Mahmood, Howard S. Smith and Brian K. McCandless

Departments of Radiology, Pediatrics and Anesthesia, Albany Medical College, Albany, New York

We evaluated the feasibility of cone-beam tomography (SPECT with a converging collimator) for detecting bone pathology of the distal extremities. **Methods:** We examined 11 patients: seven with hand or wrist pain, three with ankle pain and one with tibial pain. Cone-beam tomography was performed using a high-resolution converging collimator with a 45-cm focal length. Tomograms were then compared to high-resolution planar images. **Results:** Cone-beam tomography was successfully performed in all patients and tomograms were reconstructed in time for inclusion in the clinical report. In five patients, cone-beam tomography identified abnormalities that were equivocal or poorly defined on planar images. All other cone-beam studies provided the same information as the planar images. **Conclusions:** Tomographic imaging of the distal extremities can be successfully performed by using cone-beam tomography which has been found to be feasible and potentially useful in the clinical setting.

Key Words: cone-beam tomography; SPECT; image processing; bone scanning

J Nucl Med 1994; 35:914-917

SPECT improves image contrast over planar imaging and provides three-dimensional localization of the radiopharmaceutical (1). SPECT is typically used to examine the axial body or the proximal lower extremities, however, SPECT of the distal extremities is difficult because of low count rates and inefficient use of the camera's field of view. SPECT with a converging collimator (cone-beam tomography) offers a potential solution (2-4). Compared to a parallel-hole collimator, a converging collimator magnifies images on the camera crystal (2) and improves sensitivity at a given resolution (3,4).

The reconstruction of cone-beam tomograms is more difficult than the reconstruction of parallel-hole SPECT studies (5). We implemented cone-beam SPECT reconstruction (6) on a high-speed desktop personal computer and achieved reconstruction times that allow the use of cone-beam tomography in a clinical setting. We also developed a quality control program for implementing cone-

beam tomography. In this study, we evaluate the feasibility of cone-beam tomography for detecting bone pathology in the distal extremities.

MATERIALS AND METHODS

Patient Population

We consecutively recruited adults who were referred for bone scanning of suspected pathology of a distal extremity. We studied 11 patients ranging in age from 19 to 45 yr: 7 with hand or wrist pain, 3 with ankle pain and 1 with tibial pain. Three patients had diffuse hand pain and were referred for evaluation of reflex sympathetic dystrophy. All other patients had focal pain. The human studies committee of Albany Medical Center approved this investigation and all patients gave written informed consent.

Data Acquisition

Images were obtained 2-4 hr after intravenous injection of 20 mCi (740 MBq) of ^{99m}Tc -methylene diphosphonate. Planar images were obtained over 3-5 min using a high-resolution, parallel-hole collimator (40-cm field of view and 4.3-mm system resolution at the collimator surface) or a high-resolution converging collimator (36-cm field of view and 4.2-mm system resolution at the collimator surface). Planar images were acquired on a digital computer (ICON AP, Siemens Gammasonics, Inc.) using a 256×256 matrix.

In cone-beam tomography, we positioned the extremity in a holder made of 6.35 mm polyvinylchloride. The holder allowed the camera to rotate about the extremity in a 6-9-cm radius. To image the hand, we had the patient sit in a chair (Fig. 1). To image the foot or leg, we had the patient lay supine on an imaging table and extended his or her leg onto the holder. Data were acquired using a commercially available high-resolution converging collimator (Part #444-2620, Siemens Gammasonics, Inc.) mounted on a round-head SPECT camera which was connected to a digital computer (Orbiter 3700 and ICON AP, Siemens Gammasonics, Inc.). Data acquisition consisted of 64×64 matrix images taken for 35-40 sec at 64 stops over a 360-degree circular arc.

Quality Control

Tomographic reconstruction of cone-beam images requires measuring the focal distance of the collimator (in pixels), the camera center of rotation and the coordinates of the focal point projected on the image matrix (7,8).

We determined the converging collimator's focal length by measuring the distance from the scintillation crystal to the point of maximum count rate response to a cylindrical ^{99m}Tc point source (10 mm height \times 6 mm diameter). We calibrated pixel size by

Received Aug. 2, 1993; revision accepted Jan. 13, 1994.
For correspondence or reprints contact: Jeffrey A. Cooper, MD, Nuclear Medicine, A-72, 47 Scotland Avenue, Albany Medical Center, Albany, NY 12208.

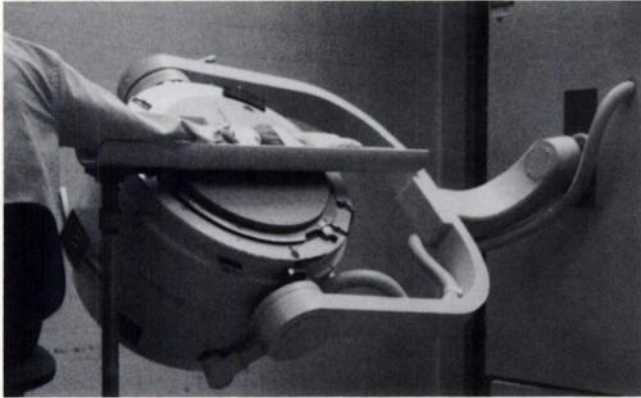


FIGURE 1. Pallet used to hold patient extremities for cone-beam imaging. The holder was designed to allow the camera to rotate in a radius as small as 6 cm.

imaging two 1-mm ^{99m}Tc point sources separated by 20 cm. We then converted the focal distance from centimeters to pixels.

The center of rotation (x_{cor}) was determined by imaging a 1-mm radius, ^{99m}Tc point source over 360° with a high-resolution, parallel-hole collimator. The average horizontal position of the point source on the image matrix was used as the center of rotation.

We determined the projection of the focal point of the converging collimator onto the detector surface (x_c, y_c) by imaging a 1-mm radius ^{99m}Tc point source over 360° with the converging collimator. We then fit the coordinates of the point source on the planar projections (x_α, y_α) into the following equations (7):

$$x_\alpha = \frac{D[(x - x_{\text{cor}}) \sin \alpha - (y - x_{\text{cor}}) \cos \alpha]}{D - (x - x_{\text{cor}}) \cos \alpha - (y - x_{\text{cor}}) \sin \alpha} + x_c, \quad \text{Eq. 1}$$

$$y_\alpha = \frac{D(z - y_c)}{D - (x - x_{\text{cor}}) \cos \alpha - (y - x_{\text{cor}}) \sin \alpha} + y_c, \quad \text{Eq. 2}$$

where x and y are the coordinates of the point source in the transaxial plane, z is the coordinate of the point source along the axis of rotation, α is the camera angle and D is the focal distance. Equations 1 and 2 were fit by allowing x_c, y_c and y_{cor} to vary to determine if the collimator affected the center of rotation. The coordinate system is the same as previously published (7) except that the detector surface coincides with the axis of rotation. The coordinates of the projection image are mirrored because the image is viewed as if looking at the back of the detector. In addition, the coordinates of the projection image are flipped because images are stored with y increasing from top to bottom.

Image Processing

Planar projections were corrected for field nonuniformity with a 30-million count extrinsic flood image. The projection data were filtered with a two-dimensional Metz filter (9) and backprojected with the Feldkamp algorithm (6). To simplify reconstruction, we assumed that the crystal was at the axis of rotation (6). This assumption magnifies images proportional to the radius of rotation (6). Filtering and backprojection were performed on a 33-MHz 80486DX computer. Attenuation and scatter correction were not performed. Transaxial images were reconstructed into coronal, sagittal, oblique and volume rendered images on an ICON AP computer (Siemens Gammasonics, Inc.) for 30 min. Cone-beam tomograms were reconstructed on the day of examination and

were interpreted by a nuclear physician who knew the patient's history and the planar image results.

RESULTS

Quality Control

The horizontal coordinate of the projection of the converging collimator's focal point (x_c) and the center of rotation (x_{cor}) coincided within 0.2 pixels. The converging collimator did not affect the center of rotation. The focal distance of the collimator (D) was 49.5 cm from the crystal surface (45 cm from the collimator face).

Clinical Results

Cone-beam tomography was successful in all patients. In five patients, cone-beam tomograms identified areas of uptake that were equivocal or not seen on planar images. In two patients, both planar and cone-beam tomograms were normal. In four patients, cone-beam tomograms and planar images provided identical information. In two patients with bone lesions that had intense uptake on planar images, axial blurring (crosstalk) was present. Otherwise, we did not see artifacts attributable to the use of cone-beam collimation.

Patient 1

A 33-yr-old female was referred for evaluation of mid-tibial pain (Figs. 2 and 3). These studies indicated tibial stress fractures and the patient recovered with conservative treatment.

Patient 2

A 42-yr-old male was referred for evaluation of right wrist pain (Figs. 4, 5 and 6). Plain wrist films and polytomography were normal and the patient was diagnosed with a trapezoid fracture.

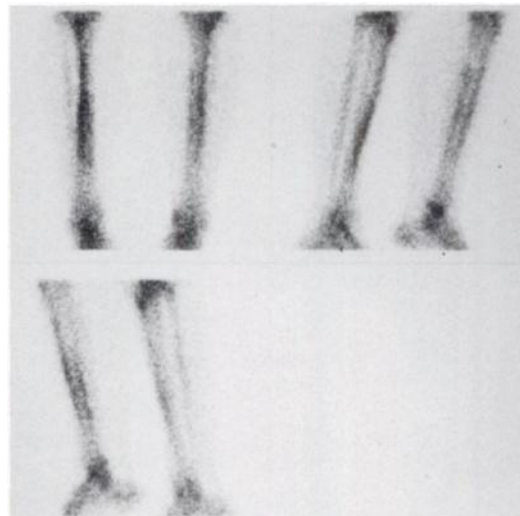


FIGURE 2. Planar ^{99m}Tc -methylene diphosphonate images of the lower legs of a patient with right tibial pain. Images, clockwise from the upper left, are anterior, right lateral and left lateral. There was mildly asymmetric activity along the cortical margins of right tibia in a pattern suggestive of stress fractures.

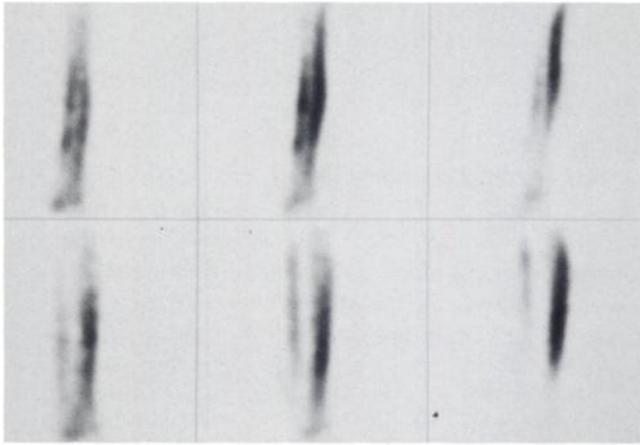


FIGURE 3. Cone-beam tomographic images of the right lower leg of the patient in Figure 1. Coronal images are in the top row and sagittal images are in the bottom row. The anterior tibial cortex demonstrated diffuse increased uptake. The posterior cortex showed two foci of increased uptake. The images defined the marrow cavity between the anterior and posterior cortices.

Patient 3

A 20-yr-old male was referred for evaluation of right wrist pain (Figs. 7 and 8). Studies demonstrated scapholunate arthritis. The patient's symptoms were resolved after injection of the scapholunate joint with steroids.

DISCUSSION

SPECT of the distal extremities has been impractical because of low count rates and inefficient use of the camera's field of view. Using cone-beam tomography solved these problems and we successfully performed practical tomographic imaging of the distal extremities in a clinical setting. To our knowledge, tomographic imaging of the distal extremities has not been previously reported.

The potential clinical utility of cone-beam tomography



FIGURE 4. Planar palmar ^{99}Tc -methylene diphosphonate images of the hand of a 42-yr-old male with right wrist pain. The planar images showed a questionable focus of increased uptake in the trapezoid region of the right hand.



FIGURE 5. Coronal cone-beam tomograms of the right hand of the patient in Figure 4. These images demonstrated focal increased uptake proximal to and aligned with the second metacarpal in the region of the trapezoid.

(3,4,7) has been limited by long reconstruction times. In the past, cone-beam reconstruction was performed on expensive main frame computers. Now, a low-cost, 66-MHz 486DX2 computer, available in many clinics, can reconstruct a cone-beam tomogram in 15 min.

Another limitation of cone-beam tomography is truncation artifact. This occurs when the organ of interest extends beyond the camera's field of view. Truncation artifacts can occur with both parallel-hole and cone-beam SPECT, but is a greater problem in cone-beam SPECT because of its smaller field of view (10). Truncation artifacts limit the utility of cone-beam tomography when imaging the axial body. We avoided truncation by restricting imaging to the distal extremities.

Parallel-hole SPECT of the distal extremities is difficult because of low count rates. Cone-beam collimators have a greater sensitivity than parallel-hole collimators with the same hole width, hole depth and septal thickness. The ratio of sensitivities is $D/(D - d)$, where D is the focal length and d is the distance between the object and the crystal (4). By enlarging the radius of rotation and distancing the object from the camera, we can increase the sensitivity as needed. Reduced resolution is the result of a larger radius of rotation. However, resolution will be reduced similarly for converging and parallel-hole collimators (4). Therefore, cone-beam tomography may be useful in imaging organs with a low photon flux.

We used a commercial collimator designed for planar imaging. Converging collimators designed for tomography

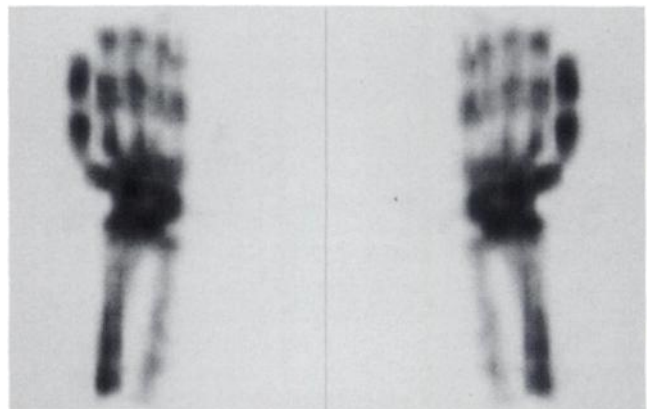


FIGURE 6. Anterior and posterior volume-rendered images of the right hand of the patient in Figures 4 and 5. These images demonstrated focal increased uptake in the region of the trapezoid.



FIGURE 7. Planar palmar ^{99m}Tc -methylene diphosphonate image of the hands of a 20-yr-old patient with right wrist pain. The planar images demonstrated irregular uptake in the proximal mid right wrist.

have more accurate hole angulation. In this study, we used very small camera orbits. An inaccurate hole angulation in small orbits where the organ is close to the camera results in less spatial error than in large radius orbits. Larger radius orbits may accentuate the inaccuracies of a low quality collimator and result in a poor reconstruction.

In our reconstruction algorithm, we assumed that the camera detector coincided with the axis of rotation (6). This decreased the time of reconstruction, but scaled the images by $D/(D - r)$ where D is the focal length and r is the radius of rotation. Since we were not interested in quantitation, we ignored this scaling factor. Recognition of this scaling factor may be important if an examination requires organ-size measurements or absolute quantitation in cpm/ml^2 .

Cone-beam SPECT reconstruction with the Feldkamp algorithm can cause artifacts that are not seen in parallel-hole imaging. One important artifact is axial blurring when the reconstructed slice moves away from the central plane of the collimator (10). We saw this artifact with lesions having intense uptake. However, this artifact did not de-



FIGURE 8. Coronal reconstructions of the cone-beam tomography study of the right hand of the patient in Figure 7. These images demonstrated focal increased uptake in the scapholunate region.

grade the diagnostic information in the cone-beam tomograms.

Simulation (11) and phantom (12) studies suggest that cone-beam tomography detects lesions better than parallel-hole tomography. However, cone-beam tomography requires more time and effort than parallel-hole tomography. Our data show that cone-beam tomography of the distal extremities is feasible and potentially useful. However, our results cannot justify replacing parallel-hole tomography with cone-beam tomography. A study directly comparing cone-beam tomography to parallel-hole tomography will be required to determine if the extra time and effort of cone-beam tomography yields an improvement over parallel-hole tomography.

CONCLUSION

Tomographic imaging of the distal extremities can be successfully performed by using cone-beam tomography. Cone-beam tomography is feasible and potentially useful in the clinical setting.

REFERENCES

- Heller SL, Goodwin PN. SPECT instrumentation: performance, lesion detection and recent innovations. *Semin Nucl Med* 1987;17:184-189.
- Gullberg GT, Zeng GL, Datz FL, Christian PE, Tung CH, Morgon HT. Review of convergent beam tomography in single photon emission computed tomography. *Phys Med Biol* 1992;37:507-534.
- Hahn LJ, Jaszczak RJ, Gullberg GT, et al. Noise characteristics for cone-beam collimators: a comparison with parallel-hole collimators. *Phys Med Biol* 1988;33:541-555.
- Jaszczak RJ, Floyd CE, Manglos SH, Greer KL, Coleman RE. Cone-beam collimation for single photon emission computed tomography: analysis, simulation, and image reconstruction using filtered backprojection. *Med Phys* 1986;13:484-489.
- Smith BD. Cone-beam tomography: recent advances and a tutorial review. *Optical Engineering* 1990;29:524-534.
- Feldkamp LA, Davis LC, Kress JW. Practical cone-beam algorithm. *Opt Soc Am* 1984;6:612-619.
- Gullberg GT, Tsui BMW, Crawford CR, Ballard JG, Hagius JT. Estimation of geometrical parameters and collimator evaluation for cone-beam tomography. *Med Phys* 1990;17:264-272.
- Li J, Wang H, Jaszczak RJ, Colman RE. A cone-beam reconstruction algorithm with a displaced center of rotation [Abstract]. *J Nucl Med* 1992;33:891.
- King MA, Doherty PW, Schwinger RB, Jacobs DA, Kidder RE, Miller TR. Fast count-dependent digital filtering of nuclear medicine images: concise communication. *J Nucl Med* 1983;24:1039-1045.
- Zeng GL, Gullberg GT. A study of reconstruction artifacts in cone-beam tomography using filtered backprojection and iterative EM algorithm. *IEEE Trans Nucl Sci* 1990;37:759-767.
- Terry JA, Tsui BMW, Perry JR, Gullberg GT. An observer evaluation study of defect detection in cardiac SPECT imaging using cone-beam geometry [Abstract]. *J Nucl Med* 1992;33:961.
- Li J, Jaszczak, Turkington TG, Metz CE, Greer KL, Coleman RE. An evaluation of lesion detectability with cone-beam, fan beam and parallel-hole SPECT by continuous ROC analysis [Abstract]. *J Nucl Med* 1993;34:81P.